# Supplementary Information

# Polyhydroxybutyrate (PHB)-based Triblock Copolymers : Synthesis of Hydrophobic PHB/Poly(benzyl β-malolactonate) and Amphiphilic PHB/Poly(malic acid) Analogues by Ring-Opening Polymerization

Ghislaine Barouti, and Sophie M. Guillaume*

Institut des Sciences Chimiques de Rennes (ISCR), UMR 6226 CNRS - Université de Rennes 1, Campus de Beaulieu, 263 Avenue du Général Leclerc, F-35042 Rennes Cedex, France

---

* Corresponding author : sophie.guillaume@univ-rennes1.fr

## Experimental section

**General conditions.**

**Instrumentation and measurements.**

**Typical procedure for the ROP of MLA$^{Be}$ using PHB-diol as a macroinitiator.**

**Typical hydrogenolysis of PMLA$^{Be}$-*b*-PHB-*b*-PMLA$^{Be}$ into PMLA-*b*-PHB-*b*-PMLA.**

**Thermogravimetric analysis (TGA) of the hydrophobic copolymers PMLA$^{Be}$-*b*-PHB-*b*-PMLA$^{Be}$ and their parent amphiphilic triblock copolymers PMLA-*b*-PHB-*b*-PMLA.**

## Table and Figures captions

**Table S1.** Ring-opening polymerization of BL promoted by HOTf/butanediol in bulk conditions at 30 °C.[3]

**Figure S1.** $^1$H NMR (400 MHz, acetone-$d_6$, 23 °C) spectrum of a HO–PHB$_{4900}$–OH sample synthesized by ROP of MLA$^{Be}$ from HOTf/butanediol (Table S1, entry 5). (* marker stands for residual water and acetone).

**Figure S2.** $^1$H NMR (400 MHz, acetone-$d_6$, 23 °C) spectrum of a HO–PMLA$^{Be}{}_{4100}$-*b*-PHB$_{2500}$-*b*-PMLA$^{Be}{}_{4100}$–OH sample synthesized by ROP of MLA$^{Be}$ from Nd(OTf)$_3$/HO–PHB$_{2100}$–OH (Table 1, entry 6) *before purification* through a silica column (* marker stands for residual water) (to be compared with the $^1$H NMR spectrum of the *purified sample,* Figure S5).

**Figure S3.**$^1$H NMR (400 MHz, acetone-$d_6$, 23 °C) spectrum of a HO–PMLA$^{Be}{}_{400}$-*b*-PHB$_{2500}$-*b*-PMLA$^{Be}{}_{400}$–OH sample synthesized by ROP of MLA$^{Be}$ from Nd(OTf)$_3$/HO–PHB$_{2700}$–OH (Table 1, entry 1) (* marker stands for residual acetone).

**Figure S4.** $^1$H NMR (400 MHz, acetone-$d_6$, 23 °C) spectrum of HO–PMLA$^{Be}{}_{500}$-*b*-PHB$_{6500}$-*b*-PMLA$^{Be}{}_{500}$–OH sample synthesized by ROP of MLA$^{Be}$ from Nd(OTf)$_3$/HO–PHB$_{6700}$–OH (Table 1, entry 2) (* marker stands for residual water and acetone).

**Figure S5.** $^1$H NMR (400 MHz, acetone-$d_6$, 23 °C) spectrum of HO–PMLA$^{Be}{}_{4100}$-*b*-PHB$_{2500}$-*b*-PMLA$^{Be}{}_{4100}$–OH sample synthesized by ROP of MLA$^{Be}$ from Nd(OTf)$_3$/HO–PHB$_{2100}$–OH (Table 1, entry 6) (* marker stands for residual water ).

**Figure S6.** $^{13}$C{$^1$H} J-MOD NMR (100 MHz, acetone-$d_6$, 23 °C) spectrum of HO–PMLA$^{Be}{}_{2200}$-*b*-PHB$_{4900}$-*b*-PMLA$^{Be}{}_{2200}$–OH synthesized by ROP of MLA$^{Be}$ from Nd(OTf)$_3$/HO–PHB$_{4900}$–OH (Table 1, entry 5).

**Figure S7.** $^1$H-$^{13}$C HMBC NMR (400 MHz, acetone-$d_6$, 23 °C) spectrum of HO–PMLA$^{Be}{}_{2200}$-*b*-PHB$_{4900}$-*b*-PMLA$^{Be}{}_{2200}$–OH synthesized by ROP of MLA$^{Be}$ from Nd(OTf)$_3$/HO–PHB$_{4900}$–OH (Table 1, entry 5).

**Figure S8.** $^1$H-$^{13}$C HSQC NMR (400 MHz, acetone-$d_6$, 23 °C) spectrum of a HO–PMLA$^{Be}{}_{2200}$-*b*-PHB$_{4900}$-*b*-PMLA$^{Be}{}_{2200}$–OH sample synthesized by ROP of MLA$^{Be}$ from Nd(OTf)$_3$/HO–PHB$_{4900}$–OH (Table 1, entry 5).

**Figure S9.** SEC chromatograms of a HO–PHB$_{4900}$–OH macroinitiator ($M_{n,SEC}$ = 5100 g.mol$^{-1}$, $Đ_M$ = 1.21; Table S1, entry 5), and of the corresponding HO–PMLA$^{Be}{}_{2200}$-*b*-PHB$_{4900}$-*b*-PMLA$^{Be}{}_{2200}$–OH triblock copolymer ($M_{n,SEC}$ = 5600 g.mol$^{-1}$, $Đ_M$ = 1.23) synthesized by the ROP of MLA$^{Be}$ promoted by the Nd(OTf)$_3$/HO–PHB$_{4900}$–OH catalytic system (Table 1, entry 5).

**Figure S10.** $^1$H NMR (400 MHz, acetone-$d_6$, 23 °C) spectrum of HO–PMLA$_{1100}$-*b*-PHB$_{4600}$-*b*-PMLA$_{1100}$–OH obtained upon hydrogenolysis of HO–PMLA$^{Be}{}_{2200}$-*b*-PHB$_{4900}$-*b*-PMLA$^{Be}{}_{2200}$–OH (Table 1, entry 5) (* marker stands for residual water and acetone). The signals of the PMLA block do not suitably integrate as the result of the partial solubility of this block in acetone.

**Figure S11.** $^1H$ NMR (400 MHz, acetone-*d₆*/TFA (98:02, *v*/*v*), 23 °C) spectrum of HO–PMLA-*b*-PHB-*b*-PMLA–OH obtained upon hydrogenolysis of HO–$PMLA^{Be}_{400}$-*b*-$PHB_{2500}$-*b*-$PMLA^{Be}_{400}$–OH (Table 1, entry 1) (* marker stands for water and residual acetone)

**Figure S12**. $^1H$ NMR (400 MHz, acetone-$d_6$/TFA (98:02, *v*/*v*), 23 °C) spectrum of HO–PMLA-*b*-PHB-*b*-PMLA–OH obtained upon hydrogenolysis of HO–$PMLA^{Be}_{500}$-*b*-$PHB_{6500}$-*b*-$PMLA^{Be}_{500}$–OH (Table 1, entry 2) (* marker stands for water and residual acetone).

**Figure S13.** $^1H$ NMR (400 MHz, acetone-$d_6$/TFA (98:02, *v*/*v*), 23 °C) spectrum of HO–PMLA-*b*-PHB-*b*-PMLA–OH obtained upon hydrogenolysis of HO–$PMLA^{Be}_{4100}$-*b*-$PHB_{2500}$-*b*-$PMLA^{Be}_{4100}$–OH (Table 1, entry 6) (* marker stands for unidentified impurities).

**Figure S14.** $^{13}C\{^1H\}$ J-MOD NMR (100 MHz, acetone-$d_6$/TFA –98:02, *v*/*v*, 23 °C) spectrum of the HO–$PMLA_{1100}$-*b*-$PHB_{4600}$-*b*-$PMLA_{1100}$–OH sample obtained upon hydrogenolysis of the HO–$PMLA^{Be}_{2200}$-*b*-$PHB_{4900}$-*b*-$PMLA^{Be}_{2200}$–OH (Table 1, entry 5) (* marker stands for unidentified impurities).

**Figure S15.** DOSY NMR (400 MHz, acetone-$d_6$, 23 °C) spectrum of HO–$PMLA_{1100}$-*b*-$PHB_{4600}$-*b*-$PMLA_{1100}$–OH obtained upon hydrogenolysis of HO–$PMLA^{Be}_{2200}$-*b*-$PHB_{4900}$-*b*-$PMLA^{Be}_{2200}$–OH (Table 1, entry 5) ($D = 102.10^{-11}$ $m.s^{-1}$).

**Figure S16.** Thermal degradation profiles of $PMLA^{Be}_{4300}$ homolymer.

**Figure S17.** Thermal degradation profiles of PMLA-*b*-PHB-*b*-PMLA copolymers: a) $PMLA^{Be}_{5200}$-*b*-$PHB_{1100}$-*b*-$PMLA^{Be}_{5200}$, b) $PMLA^{Be}_{1200}$-*b*-$PHB_{1700}$-*b*-$PMLA^{Be}_{1200}$, c) $PMLA_{600}$-*b*-$PHB_{1700}$-*b*-$PMLA_{600}$, c) $PMLA_{2600}$-*b*-$PHB_{1100}$-*b*-$PMLA_{2600}$ (Table 1, entries 4, 7, ESI†).

**Figure S18.** DSC trace (second heating cycle; heating rate = 10 $°C.min^{-1}$; helium flow) of $PMLA^{Be}_{5200}$-*b*-$PHB_{1100}$-*b*-$PMLA^{Be}_{5200}$ (Table 1, entry 7).

## Experimental section

**General conditions.** All polymerizations were performed under inert atmosphere (argon, < 3 ppm $O_2$) using standard Schlenk, vacuum line, and glovebox techniques. Toluene was dried over a mixture of 3 and 4 Å molecular sieves. *Racemic* benzyl β-malolactonate ($MLA^{Be}$) was synthesized from (D,L)-aspartic acid according to the literature procedure.[1,2] Butane-1,4-diol (Aldrich, 99%) was dried over a mixture of 3 and 4 Å molecular sieves and stored under argon atmosphere. Neodymium triflate $Nd(OTf)_3$, trifluoromethanesulfonic acid (triflic acid, $CF_3SO_3H$, HOTf, $\geq$ 99%), palladium on activated charcoal (10%), 1,5,7-triazabicyclo[4.4.0]dec-5-ene (TBD) (98%) and all other reagents were used as received (Aldrich unless otherwise mentioned). PHB diols were synthesized by the ROP of β-butyrolactone (BL) mediated by HOTf/butane diol according to the reported procedure;[3] it was further purified in the present work by dialysis using acetone (800 mL, renewed twice) and characterized by $^1H$ NMR in agreement with literature data (Table S1, Figure S1). $PMLA^{Be}$ was synthesized by ROP of $MLA^{Be}$ mediated by TBD as previously described[4] and then purified by dialysis in acetone. Spectra/Por dialysis membranes with a molecular weight cut off (MWCO) of 1000 or 3500 $g.mol^{-1}$ (nominal flat width = 45 mm, diameter = 29 mm, volume/length = 15 m/50 ft) were purchased from Spectrumlabs.

**Instrumentation and measurements.** $^1H$ (400 MHz), $^{13}C\{^1H\}$ J-MOD (100 MHz), 2D $^1H$-$^{13}C$ HSQC, $^1H$-$^{13}C$ HMBC and DOSY NMR spectra were recorded on Bruker Ascend 400 spectrometers at 25 °C in acetone-$d_6$, and were referenced internally relative to $SiMe_4$ ($\delta$ 0 ppm) using the residual solvent resonances. DOSY spectra were acquired in acetone-$d_6$ with the *stebpgp1s* pulse program from Bruker topspin software. All spectra were recorded with 32 K time domain data points in the $t_2$ dimension and 32 $t_1$ increments. The gradient strength was logarithmically incremented in 32 steps from 2% up to 95% of the maximum gradient strength. Diffusion times of 50 ms and the maximum bipolar gradient pulse length of 1.6 ms were used in order to ensure full signal attenuation. The data were processed using an SI F2 and SI F1 of 32 K. The diffusion dimension of the 2D DOSY spectra was processed by means of Bruker topspin software (version 2.1). The DOSY maps were obtained with MestReNova software (version 2.1).

Monomer conversions were calculated from $^1$H NMR spectra of the crude PMLA$^{Be}$-*b*-PHB-*b*-PMLA$^{Be}$ copolymer samples in acetone-$d_6$ by using the integration (Int.) ratio Int.$_{PMLABe}$/[Int.$_{PMLABe}$ + Int.$_{MLABe}$] of the methine hydrogen ($-OC\mathit{H}(CO_2Be)CH_2$: $\delta_{PMLABe}$ 5.50 ppm, $\delta_{MLABe}$ 4.73 ppm) of MLA$^{Be}$/PMLA$^{Be}$ (Table 1).

The molar mass values of PMLA$^{Be}$-*b*-PHB-*b*-PMLA$^{Be}$ copolymers samples were determined by $^1$H NMR analysis in acetone-$d_6$, from the relative intensities of the signals of the main-chain BL-methylene hydrogens and MLA$^{Be}$-phenyl hydrogens ($-OCH(CH_3)C\mathit{H_2}C(O)$, $\delta$ 2.57 ppm; $-OCH(CO_2CH_2\mathit{Ph})CH_2C(O)$, $\delta$ 7.37 ppm), to the methylene hydrogens of the central tetramethylene moiety ($-O(C\mathit{H_2})_4\mathit{O}$, $\delta$ 4.11 and 1.70 ppm ) (Figures 1, S3, S4, S5, S6; Table 1). Note that these latter two signals correspond to a significant number of hydrogens from the initiator and thus emerge well (in particular the methylene signal at $\delta$ 4.11 ppm) from the spectrum baseline, thereby allowing a fairly reliable integration of the resonances. Theoretical molar mass values of HO–PMLA$^{Be}$-*b*-PHB-*b*-PMLA$^{Be}$–OH copolymers were calculated from the relation: $\{[MLA^{Be}]_0/[PHB\text{-diol}]_0 \times \text{Conv.}_{MLABe} \times M_{MLABe}\}$, with $M_{MLABe} = 206$ g.mol$^{-1}$, and from $M_{NMR,OH\text{-}PHB\text{-}OH}$ (Table 1). Note also that to obtain the exact molar mass of the HO–PMLA$^{Be}$-*b*-PHB-*b*-PMLA$^{Be}$–OH, the PMLA$^{Be}$-PHB-PMLA$^{Be}$ $M_{n,NMR}$ value (Table 1) should be incremented by the molecular weight of the two chain-ends and of the tetramethylene moiety, namely $M_H = 1$ g.mol$^{-1}$ and $M_{O(CH2)4O} = 88$ g.mol$^{-1}$ (*i.e.* HO–PMLA$^{Be}$-*b*-PHB-*b*-PMLA$^{Be}$–OH $M_{n,theo}$ = PMLA$^{Be}$-*b*-PHB-*b*-PMLA$^{Be}$ $M_{n,theo}$ + 90 g.mol$^{-1}$).

The molar mass values of the PHB segment in PMLA-*b*-PHB-*b*-PMLA copolymers samples were determined by $^1$H NMR analysis in acetone-$d_6$, from the relative intensities of the signals of the main-chain methylene hydrogens ($–OCH(CH_3)CH_2C(O)$, δ 2.57 ppm), relative to the methylene hydrogens of tetramethylene moiety ($–O(CH_2)_4O$, δ 4.11 and 1.70 ppm) (Table 1).

Number-average molar mass ($M_{n,SEC}$) and dispersity ($Đ_M = M_w/M_n$) values of the (co)polymers were determined by size-exclusion chromatography (SEC) in THF at 30 °C (flow rate 1.0 mL.min$^{–1}$) on a Polymer Laboratories PL50 apparatus equipped with a refractive index detector and a set of two ResiPore PLgel 3 µm MIXED-D 300 × 7.5 mm columns. The polymer samples were dissolved in THF (2 mg.mL$^{–1}$). All elution curves were calibrated with 10 monodisperse polystyrene standards ($M_n$ range from 580 to 380,000 g·mol$^{–1}$). Note that SEC molar mass values of the (co)polymers reported in Table 1 and Table S1 are only informative relatively to one another since the hydrodynamic radius of the copolymers is possibly different from that of polystyrene standards used for the calibration. The SEC traces of the (co)polymers all exhibited a unimodal, yet non-Gaussian-shaped peak tailing at longer elution times, as exemplified with the SEC chromatograms of OH–PMLA$^{Be}_{2200}$-*b*-PHB$_{4900}$-*b*-PMLA$^{Be}_{2200}$–OH (Figure S9); this is reminiscent of previous reports on PMLA/PHB copolymers.[4,5,6,7,8]

Thermogravimetric analyses (TGA) were performed on a Metler Toledo TGA/DSC1 by heating polymer samples at a rate of 10 °C.min$^{–1}$ from +25 °C to +500 °C in a dynamic nitrogen atmosphere (flow rate = 50 mL.min$^{–1}$) (Figures 4, S16).

Differential scanning calorimetry (DSC) analyses were performed on a Setaram DSC 131 apparatus calibrated with indium at a rate of 10 °C·min$^{–1}$, under continuous flow of helium (25 mL·min$^{–1}$), using aluminum capsules. The thermograms were recorded according to the following cycles: −50 to +100 °C at 10 °C·min$^{-1}$; +100 to −50 °C at 10 °C·min$^{-1}$; −50 °C for 5 min; −50 to +100 °C at 10 °C·min$^{-1}$; +100 to −50 °C at 10 °C·min$^{-1}$.

**Typical procedure for the ROP of MLA$^{Be}$ using PHB-diol as a macroinitiator.** In a typical experiment (Table 1, entry 5), HO−PHB−OH (500 mg, 0.1 mmol, 1 equiv., $M_{n,NMR}$= 4900 g.mol$^{-1}$ (Table S1, entry 5); [PHB-diol]$_0$ = 0.1 M) was charged in a Schenk flask in the glovebox and dissolved in dry toluene (1 mL) prior to the addition of Nd(OTf)$_3$ (60 mg, 0.1 mmol, 1 equiv.). The polymerization was performed at 60 °C in a very small amount of toluene, yet sufficient enough to afford a suitable homogeneous reaction medium for the ROP of this highly viscous monomer to proceed. The mixture was next stirred for 10 min, and MLA$^{Be}$ (505 mg, 0.24 mmol, 24 equiv) was then added in. The resulting mixture was then stirred at 60 °C for 40 h (the reaction time was not systematically optimized). The polymerization was then stopped upon addition of an excess of acetone (*ca.* 2 mL), and the resulting mixture was concentrated to dryness under vacuum. MLA$^{Be}$ conversion was then determined from $^1$H NMR analysis of this residue in acetone-$d_6$. The crude polymer was next dissolved in acetone (5 mL) and dialyzed for 48 h with a dialysis membrane (MWCO of 3500 g.mol$^{-1}$) using acetone (800 mL) which was renewed twice. The resulting polymer solution (recovered inside the membrane) was finally purified through a silica column using acetone (10 mL) as eluent and finally dialyzed once more as described above. The recovered polymer was dried under vacuum overnight (0.90 g, 89 wt%) and then analyzed by SEC, $^1$H, $^{13}$C{$^1$H} J-MOD, $^1$H-$^{13}$C HSQC, $^1$H-$^{13}$C HMBC, and DOSY NMR in acetone-$d_6$, and TGA as HO−PMLA$^{Be}$-*b*-PHB-*b*-PMLA$^{Be}$−OH (Figures 1−2, 4, S3−S9). The copolymer samples were stored under inert atmosphere at 4 °C.

$^1$H NMR (400 MHz, acetone-$d_6$, 23 °C): δ (ppm) BL (–OCH(CH$_3$)C*H$_2$*C(O): 2.57, (–OC*H*(CH$_3$)CH$_2$C(O): 5.18, –OCH(C*H$_3$*)CH$_2$C(O): 1.26), MLA$^{Be}$ (–

$\mathrm{OCH(CO_2CH_2}\mathit{Ph}\mathrm{)CH_2C(O)}$: 7.37, $\mathrm{–OC}\mathit{H}\mathrm{(CO_2CH_2Ph)CH_2C(O)}$: 5.53, $\mathrm{–OCH(CO_2C}\mathit{H_2}\mathrm{Ph)CH_2C(O)}$: δ 5.21, $\mathrm{–OCH(CO_2CH_2Ph)C}\mathit{H_2}\mathrm{C(O)}$: δ 3.18), tetramethylene central moiety ($\mathrm{–O(C}\mathit{H_2}\mathrm{)_4O}$: 4.11, 1.70) (Figure 1).

$^{13}\mathrm{C}\{^1\mathrm{H}\}$ J-MOD NMR (100 MHz, acetone-*d*$_6$, 23 °C): δ (ppm) PHB ($\mathrm{O}\mathit{C}\mathrm{H(CH_3)CH_2C(O)}$, 68.5; $\mathrm{OCH(}\mathit{C}\mathrm{H_3)CH_2C(O)}$, 19.9; $\mathrm{OCH(CH_3)}\mathit{C}\mathrm{H_2C(O)}$, 41.6; $\mathrm{OCH(CH_3)CH_2}\mathit{C}\mathrm{(O)}$, 169.9); PMLA$^{\mathrm{Be}}$ ($\mathrm{O}\mathit{C}\mathrm{HC(O)OCH_2Ph)CH_2C(O)}$, 68.5; $\mathrm{OCH}\mathit{C}\mathrm{(O)OCH_2Ph)CH_2C(O)}$, 168.7; $\mathrm{OCHC(O)O}\mathit{C}\mathrm{H_2Ph)CH_2C(O)}$, 67.8; $\mathrm{OCHC(O)OCH_2}\mathit{C}\mathrm{_6H_5)CH_2C(O)}$, 136.7, 129.2) $\mathrm{OCHC(O)O}\mathit{C}\mathrm{H_2Ph)CH_2C(O)}$, 41.3; $\mathrm{OCHC(O)OCH_2Ph)CH_2}\mathit{C}\mathrm{(O)}$, 170.2; tetramethylene central moiety ($\mathrm{O}\mathit{C}\mathrm{H_2(CH_2)_2CH_2O}$, 65.2; $\mathrm{OCH_2(}\mathit{C}\mathrm{H_2)_2CH_2O}$, 26.5) (Figures S6).

**Typical hydrogenolysis of PMLA$^{\mathrm{Be}}$-*b*-PHB-*b*-PMLA$^{\mathrm{Be}}$ into PMLA-*b*-PHB-*b*-PMLA.** In a typical hydrogenolysis reaction, the isolated HO–PMLA$^{\mathrm{Be}}$-*b*-PHB-*b*-PMLA$^{\mathrm{Be}}$–OH copolymer (900 mg, 0.10 mmol, $M_{\mathrm{n,NMR}}$ = 9300 g.mol$^{-1}$) (Table 1, entry 5) was dissolved in acetone (10 mL) at room temperature in a stainless-steel autoclave prior to the addition of Pd/C (250 mg, 28 wt%). The reactor was sealed, flushed several times with $H_2$, and finally placed under $H_2$ pressure (25 bar). The reaction mixture was then allowed to stir at room temperature for 48 h, and the reactor was next vented to atmospheric pressure. The crude reaction mixture was then filtrated through Celite using acetone (200 mL) as eluent to remove the Pd/C catalyst. Solvent evaporation from the resulting clear filtrate under vacuum then afforded a viscous colorless oil. Dialysis in acetone of the resulting copolymer was next carried out as described above for HO–PMLA$^{\mathrm{Be}}$-*b*-PHB-*b*-PMLA$^{\mathrm{Be}}$–OH . The final copolymer sample, recovered as a colorless oil (600 mg, 67 wt%), was then analyzed by $^1$H, $^{13}\mathrm{C}\{^1\mathrm{H}\}$J-MOD and DOSY NMR in acetone-*d*$_6$/TFA (98:02, *v/v*) and TGA (Figures 2–3, S10–S16). The theoretical molar mass of the PHB block (*not including* the central tetramethylene moiety) was evaluated from the initial molar mass value of the PHB segment in the PMLA$^{\mathrm{Be}}$-*b*-PHB-*b*-PMLA$^{\mathrm{Be}}$ copolymers as determined by $^1$H NMR analysis (PMLA$^{\mathrm{Be}}$-

*b*-PHB-*b*-PMLA$^{Be}$, $M_{n,NMR}$; Table 1). The theoretical molar mass value of the PMLA blocks was based on the loss of the benzyl units ($M_{CH2Ph}$ = 91 g.mol$^{-1}$). Since this depletion amounts to roughly half the molar mass of the MLA$^{Be}$ units ($M_{MLABe}$ = 206 g.mol$^{-1}$), the molar mass of (only) the PMLA$^{Be}$ segments was simply divided by two (Table 1). Note that in the case of the HO–PMLA-*b*-PHB-*b*-PMLA–OH copolymers, the more precise theoretical molar mass was obtained upon incrementing PMLA-*b*-PHB-*b*-PMLA $M_{n,theo}$ by the molar mass of the two hydrogen chain-end and of the central tetramethylene moiety (with $M_H$ = 1 g.mol$^{-1}$ and $M_{O(CH2)4O}$ = 88 g.mol$^{-1}$; *i.e.* HO–PMLA-*b*-PHB-*b*-PMLA–OH $M_{n,theo}$ = PMLA-*b*-PHB-*b*-PMLA $M_{n,theo}$ + 90 g.mol$^{-1}$).

$^1$H NMR (400 MHz, acetone-$d_6$/TFA (98:02, *v/v*), 23 °C): δ (ppm) BL (–OC*H*($CH_3$)$CH_2$C(O): 5.24, –OCH($CH_3$)C$H_2$C(O): 2.57, (–OCH(C$H_3$)$CH_2$C(O): 1.23), MLA$^{Be}$ (COO*H*: 8.50, –OC*H*($CO_2$H)$CH_2$C(O): 5.53, –OCH($CO_2$H)C$H_2$C(O): 2.98), tetramethylene central moiety (–O(C$H_2$)$_4$O: 4.11, 1.70) (Figure 3).

$^{13}$C{$^1$H} J-MOD NMR (100 MHz, acetone-$d_6$/TFA –98:02, *v/v*, 23 °C): δ (ppm) PMLA (O*C*H(COOH)$CH_2$C(O), 68.4, OCH(*C*OOH)$CH_2$C(O), 158.7; OCH(COOH)*C*$H_2$C(O), 41.2; OCH(COOH)$CH_2$*C*(O), 169.9), PHB (O*C*H($CH_3$)$CH_2$C(O), 68.5; OCH(*C*$H_3$)$CH_2$C(O), 19.9; OCH($CH_3$)*C*$H_2$C(O), 41.6; OCH($CH_3$)$CH_2$*C*(O), 169.9), tetramethylene central moiety (O(*C*$H_2$)$_4$O, 64.2, 25.3) (Figure S14).

**Thermogravimetric analysis (TGA) of the hydrophobic copolymers PMLA$^{Be}$-*b*-PHB-*b*-PMLA$^{Be}$ and their parent amphiphilic triblock copolymers PMLA-*b*-PHB-*b*-PMLA.** The thermal properties of the hydrophobic copolymers PMLA$^{Be}$-*b*-PHB-*b*-PMLA$^{Be}$ and their parent amphiphilic triblock copolymers PMLA-*b*-PHB-*b*-PMLA were investigated by thermogravimetric analysis (TGA) (Figure 4). PMLA-*b*-PHB-*b*-PMLA copolymers remained stable up to *ca.* 155 °C while the onset of the degradation temperature of PMLA$^{Be}$-*b*-PHB-*b*-PMLA$^{Be}$ was observed at *ca.* 190 °C. The former copolymers were fully degraded at *ca.*

340 °C, while the latter copolymers reached *ca.* 90% weight loss at *ca.* 500 °C. In comparison, the parent diblock copolymers PHB-*b*-PMLA featuring a similar hydrophilic fraction (*f* 42, 82) were stable up to ca 175 °C and fully degraded at *ca.* 290 °C.[7] Similarly to PMLA-*b*-PHB diblock copolymers,[7] both sets of triblock copolymers exhibited a stepwise degradation profile. The first step occurring between *ca.* 150–280 °C for PMLA/PHB, and 180–255 °C for $\mathrm{PMLA^{Be}}$/PHB, was ascribed to the degradation of first the $\mathrm{PMLA^{(Be)}}$ segment (PMLA: $T_{d,41}^{50}$ = *ca.* 265 °C; $T_{d,83}^{50}$ = *ca.* 190 °C; $\mathrm{PMLA^{Be}}$: $T_{d,41}^{50}$ = *ca.* 230 °C; $T_{d,83}^{50}$ = *ca.* 235 °C; where $T_{d,f}^{50}$ is the temperature at which 50% of segmental mass loss occurs for the copolymer with a hydrophilic fraction of *f*). For reference, the thermogram of a homopolymer $\mathrm{PMLA^{Be}}_{4300}$ revealed it stability up to *ca.* 160 °C with complete degradation observed at *ca.* 235 °C and $T_d^{50}$ = *ca.* 210 °C (Figure S16). The second step occurring between *ca.* 265–345 °C for PMLA/PHB and above 250 °C for $\mathrm{PMLA^{Be}}$/PHB, was attributed to the degradation of the PHB segment (PMLA: $T_{d,41}^{50} \approx T_{d,83}^{50}$ = *ca.* 310 °C; $\mathrm{PMLA^{Be}}$: $T_{d,41}^{50} \approx T_{d,83}^{50}$ = *ca.* 425 °C). Note that the degradation profile corresponding to the hydrophilic block of the $\mathrm{PMLA_{600}}$-*b*-$\mathrm{PHB_{1700}}$-*b*-$\mathrm{PMLA_{600}}$ copolymer is characteristic of a very fast degradation of the polymer due to the small PMLA segment length (Figure 4c).

The thermal characteristics of the copolymer were also analyzed by DSC. The second heating cycle of the $\mathrm{PMLA^{Be}}_{5200}$-*b*-$\mathrm{PHB_{1100}}$-*b*-$\mathrm{PMLA^{Be}}_{5200}$ copolymer showed two glass transition temperatures ($T_g$) around −1 °C and +26 °C corresponding to the PHB and the $\mathrm{PMLA^{Be}}$ segments, respectively, as illustrated Figure S17. The presence of two $T_g$ nicely supported the block structure of the copolymer. The values were found close from the one previously observed with $\mathrm{PMLA^{Be}}$-*b*-PHB diblock copolymers.[4]

**Table S1.** Ring-opening polymerization of BL promoted by HOTf/butanediol in bulk conditions at 30 °C.[3]

| **Entry** | **$[BL]_0$:$[BD]_0$: $[HOTf]_0$ [a]** | **Reaction Time [b] (min)** | **BL Conv. [c] (%)** | **PHB $M_{n,theo}$ [d] ($g.mol^{-1}$)** | **PHB $M_{n,NMR}$ [e] ($g.mol^{-1}$)** | **PHB $M_{n,sec}$ [f] ($g.mol^{-1}$)** | **$Đ_M$ [g]** |
|---|---|---|---|---|---|---|---|
| 1 | 17:1:2 | 20 | 100 | 1500 | 1400 | 1700 | 1.22 |
| 2 | 27:1:2 | 30 | 100 | 2300 | 2100 | 2700 | 1.28 |
| 3 | 29:1:2 | 30 | 98 | 2500 | 2700 | 2900 | 1.27 |
| 4 | 47:1:2 | 50 | 100 | 4000 | 3800 | 4100 | 1.26 |
| 5 | 60:1:2 | 70 | 97 | 5000 | 4900 | 5100 | 1.21 |
| 6 | 78:1:2 | 77 | 100 | 6700 | 6700 | 8200 | 1.28 |

[a] All reactions were performed in bulk conditions. [b] Reaction times were not necessarily optimized. [c] BL conversion as determined by $^1H$ NMR spectroscopy of the crude reaction mixture calculated from the integration (Int.) ratio $Int._{PHB}/[Int._{PHB} + Int._{BL}]$. [d] Theoretical molar mass values of the HO–PHB–OH calculated from the relation $\{[BL]_0/[BD]_0 \times Conv._{BL} \times M_{BL}\}$, $M_{BL} = 86$ $g.mol^{-1}$. [e] Molar mass values determined by $^1H$ NMR analysis of the isolated HO–PHB–OH in acetone-$d_6$ at 25 °C, from the resonance of the terminal $-CH_2OH$ group (*not including* either the hydrogen chain-ends or the $-O(CH_2)_4O-$ central moiety). [f] Number-average molar mass values determined by SEC analysis in THF at 30 °C *vs.* polystyrene standards (uncorrected *M*n values; refer to the Experimental Section).

[g] Dispersity determined by SEC analysis in THF at 30 °C.

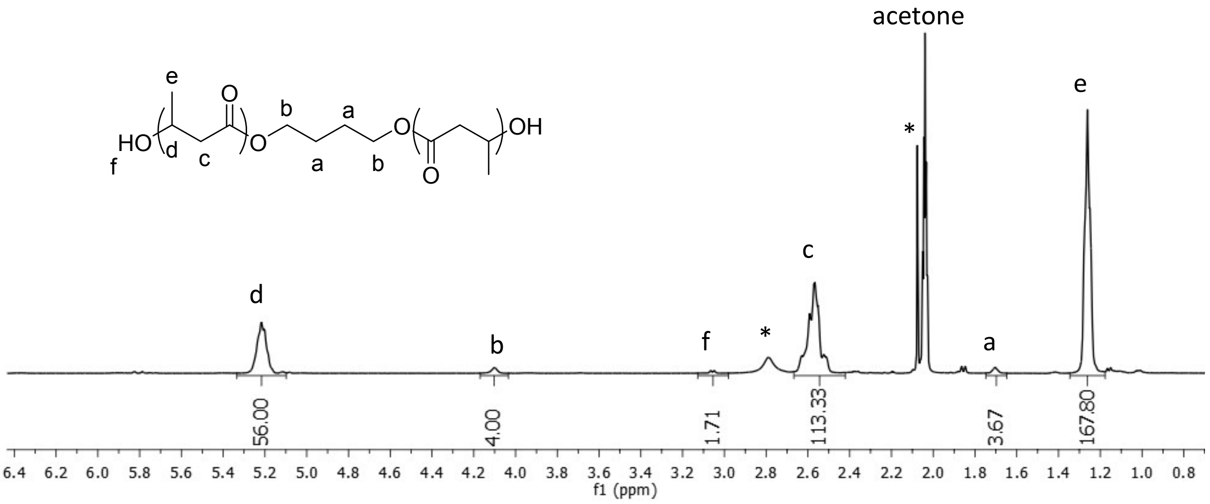

**Figure S1.** $^1$H NMR (400 MHz, acetone-$d_6$, 23 °C) spectrum of a HO–PHB$_{4900}$–OH sample synthesized by ROP of MLA$^{Be}$ from HOTf/butanediol (Table S1, entry 5). (* marker stands for residual water and acetone).

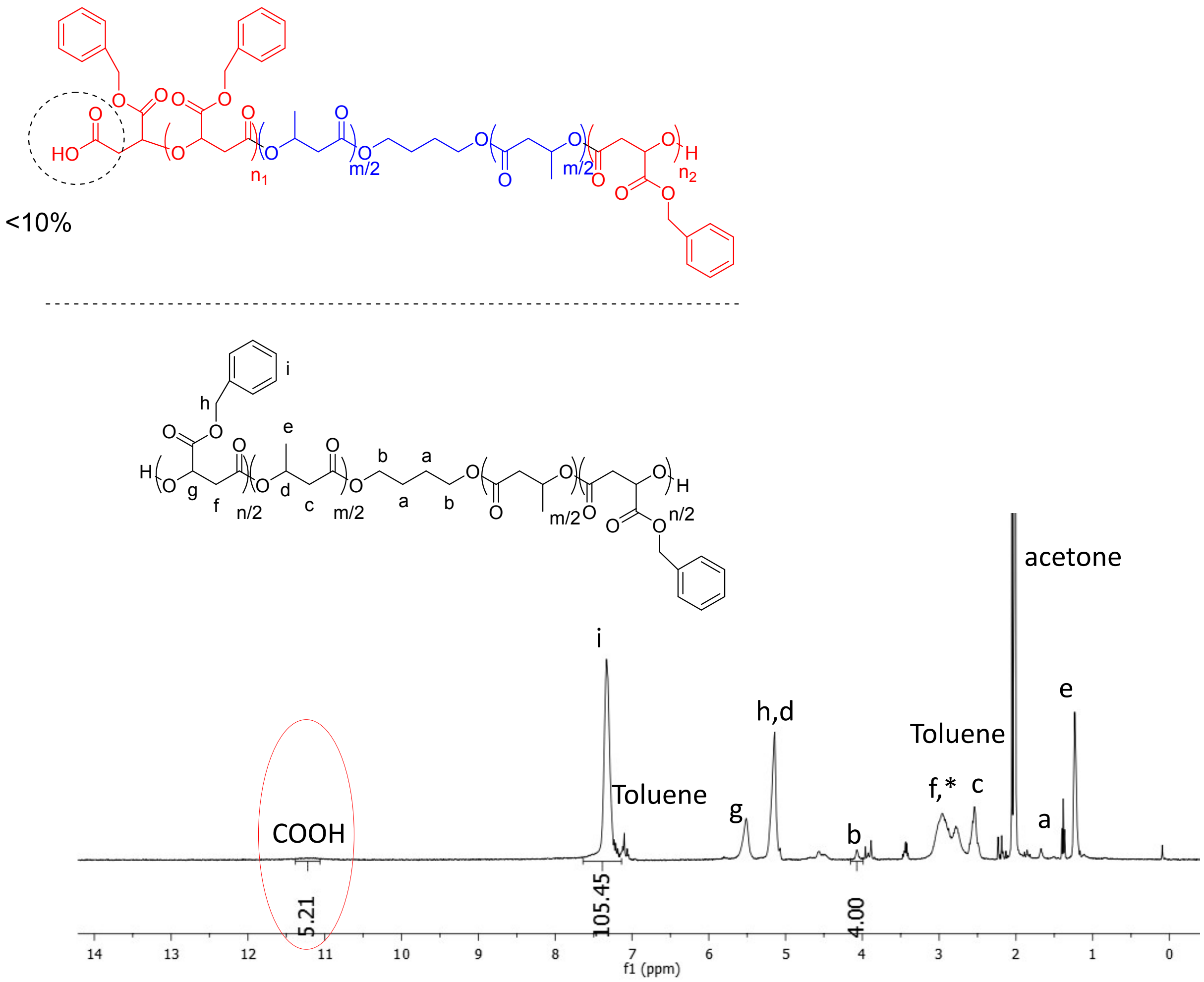

**Figure S2.** $^1$H NMR (400 MHz, acetone-$d_6$, 23 °C) spectrum of a HO–PMLA$^{Be}{}_{4100}$-*b*-PHB$_{2500}$-*b*-PMLA$^{Be}{}_{4100}$–OH sample synthesized by ROP of MLA$^{Be}$ from Nd(OTf)$_3$/HO–PHB$_{2100}$–OH (Table 1, entry 6) *before purification* through a silica column (* marker stands for residual water) (to be compared with the $^1$H NMR spectrum of the *purified sample,* Figure S5). Since the signal of the carboxylic acid integrates for 5.21 relative to the central tetramethylene moiety while 55 MLA$^{Be}$ units were consumed, there is less than 10% of carboxylic acid chain-end in the whole copolymer.

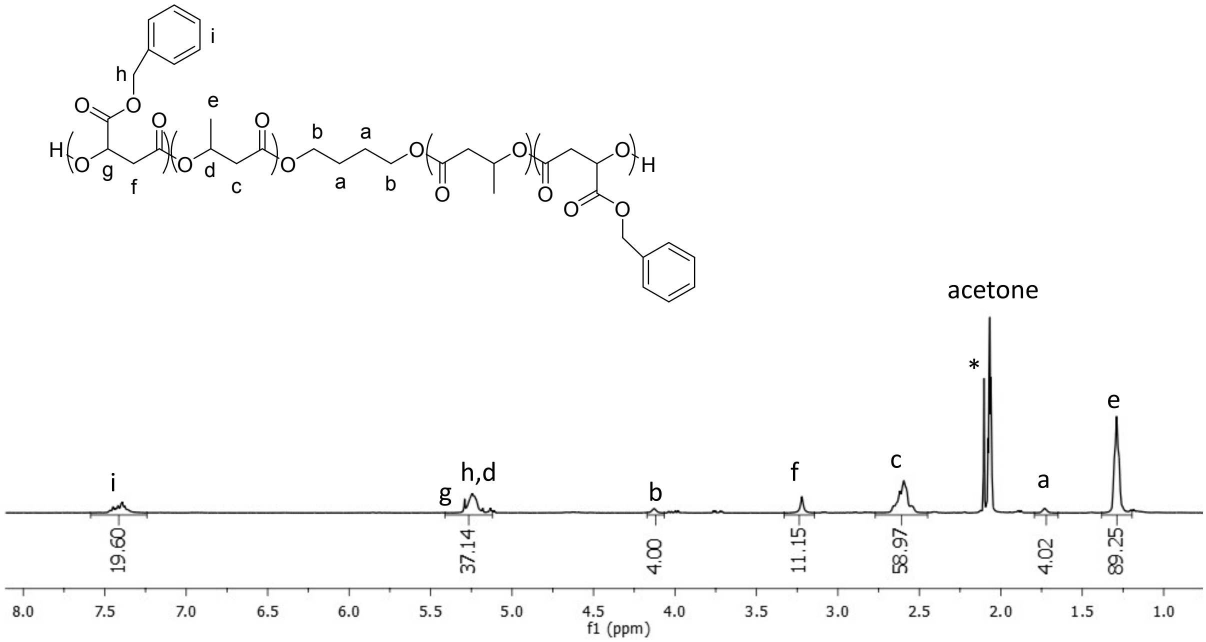

**Figure S3.**${}^{1}H$ NMR (400 MHz, acetone-$d_6$, 23 °C) spectrum of a HO–PMLA$^{Be}{}_{400}$-*b*-PHB$_{2500}$-*b*-PMLA$^{Be}{}_{400}$–OH sample synthesized by ROP of MLA$^{Be}$ from Nd(OTf)$_3$/HO–PHB$_{2700}$–OH (Table 1, entry 1) (* marker stands for residual acetone).

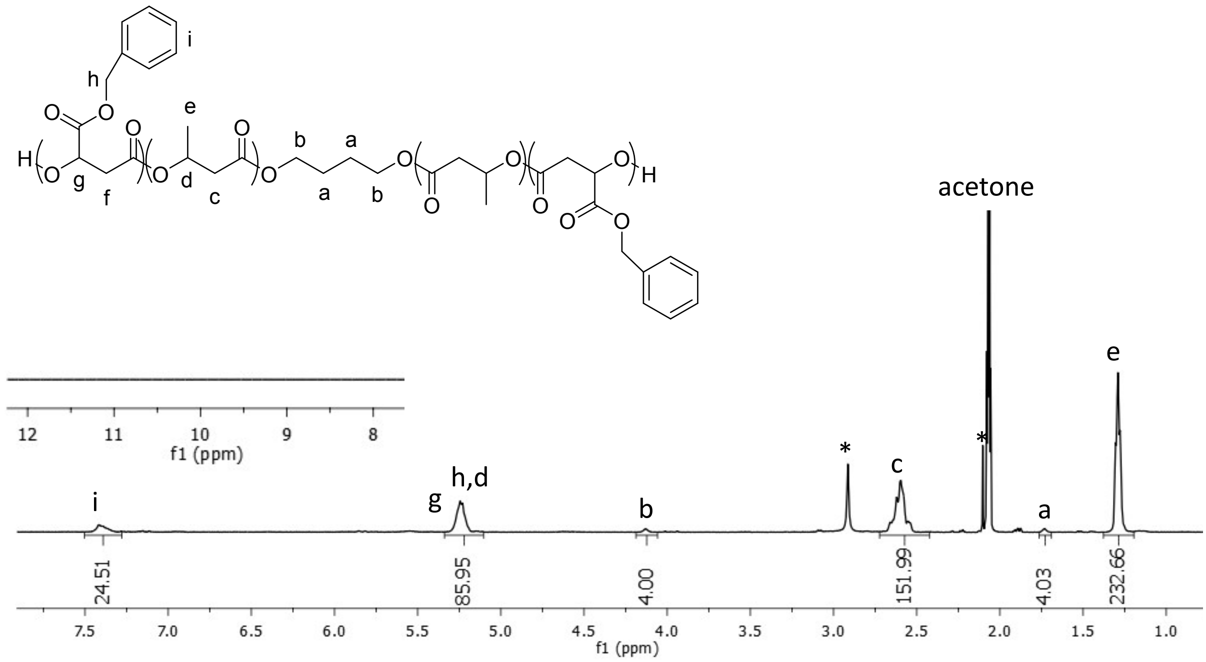

**Figure S4.** ${}^{1}H$ NMR (400 MHz, acetone-$d_6$, 23 °C) spectrum of HO–PMLA$^{Be}{}_{500}$-*b*-PHB$_{6500}$-*b*-PMLA$^{Be}{}_{500}$–OH sample synthesized by ROP of MLA$^{Be}$ from Nd(OTf)$_3$/HO–PHB$_{6700}$–OH (Table 1, entry 2) (* marker stands for residual water and acetone).

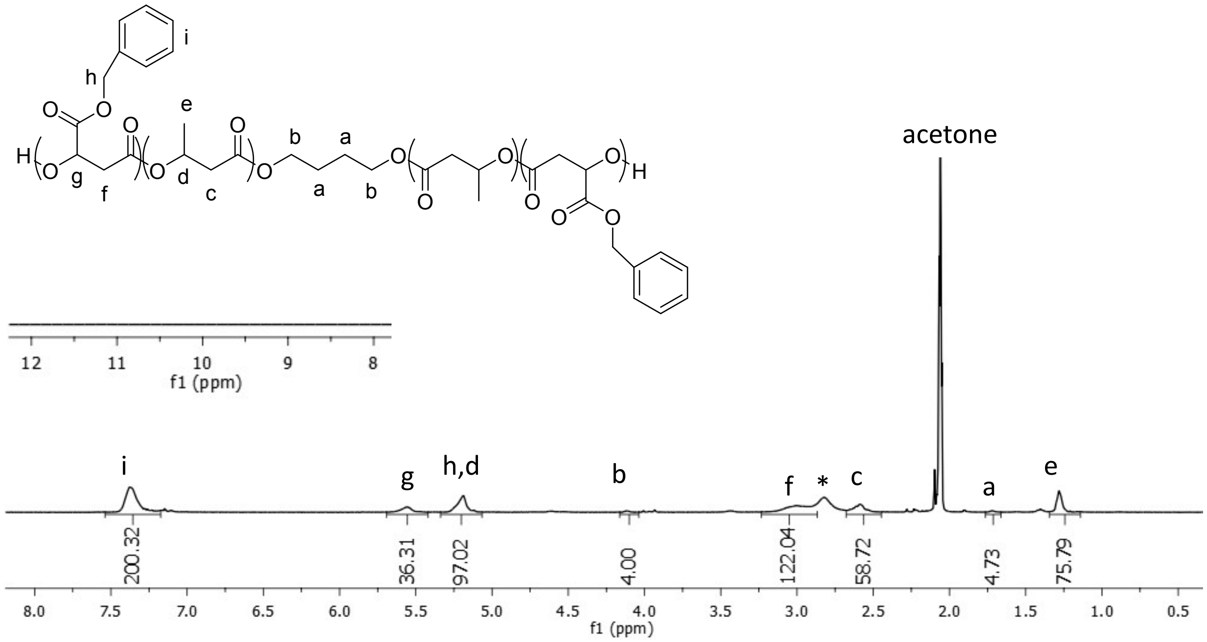

**Figure S5.** $^{1}$H NMR (400 MHz, acetone-$d_6$, 23 °C) spectrum of HO–PMLA$^{Be}_{4100}$-*b*-PHB$_{2500}$-*b*-PMLA$^{Be}_{4100}$–OH sample synthesized by ROP of MLA$^{Be}$ from Nd(OTf)$_3$/HO–PHB$_{2100}$–OH (Table 1, entry 6) (* marker stands for residual water ).

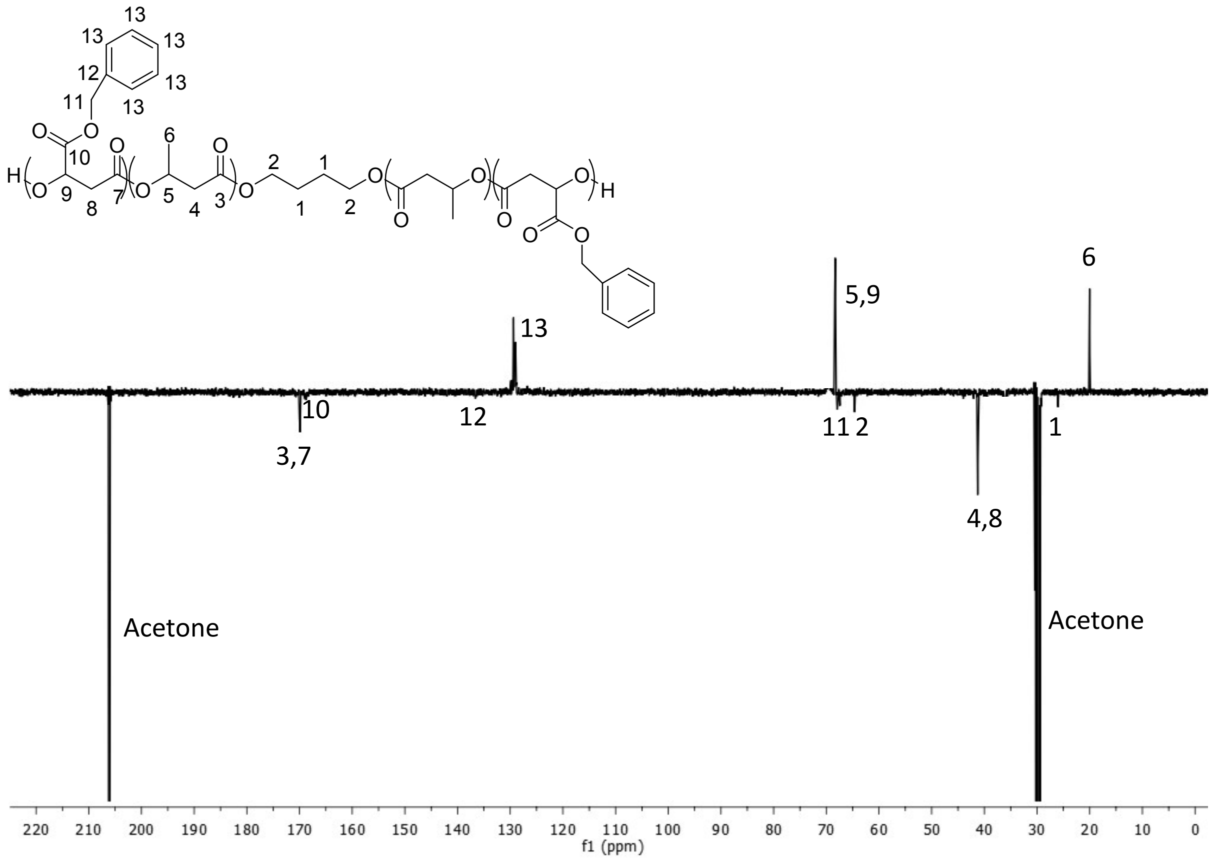

**Figure S6.** $^{13}C\{^{1}H\}$ J-MOD NMR (100 MHz, acetone-$d_6$, 23 °C) spectrum of HO–PMLA$^{Be}{}_{2200}$-*b*-PHB$_{4900}$-*b*-PMLA$^{Be}{}_{2200}$–OH synthesized by ROP of MLA$^{Be}$ from Nd(OTf)$_3$/HO–PHB$_{4900}$–OH (Table 1, entry 5).

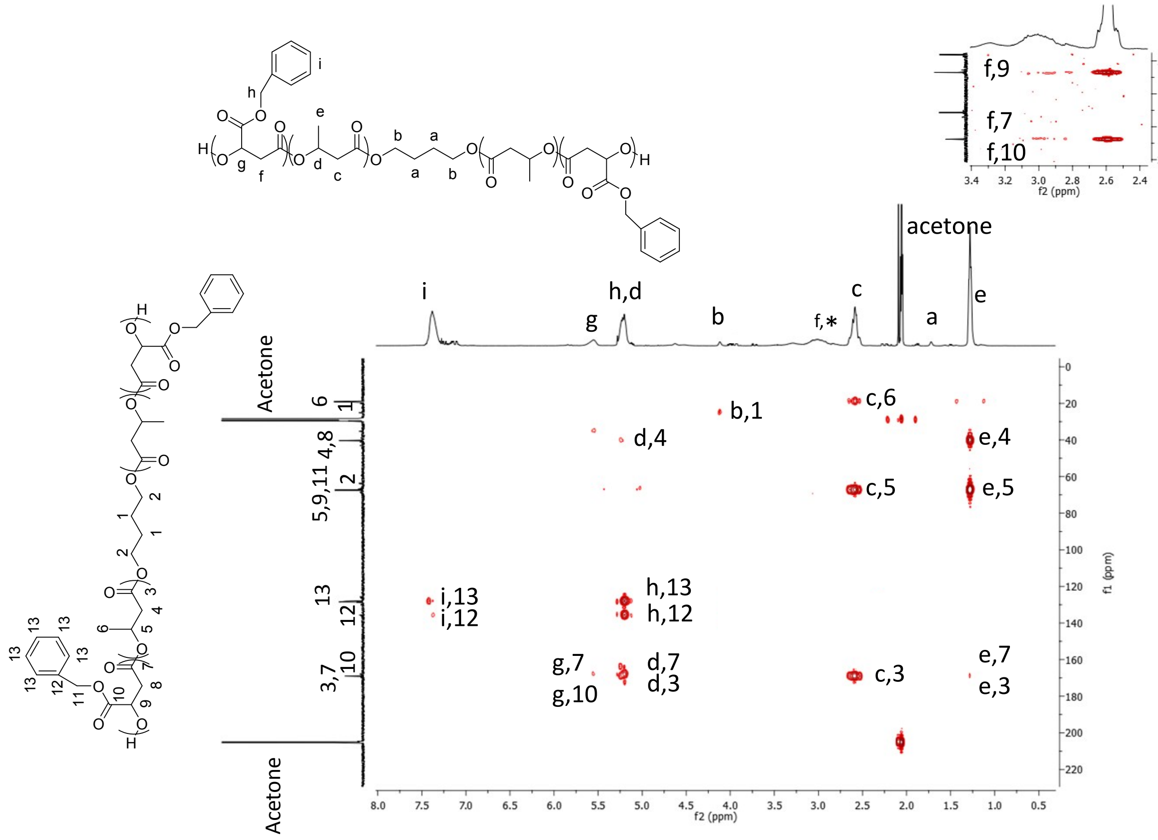

**Figure S7.** $^1$H-$^{13}$C HMBC NMR (400 MHz, acetone-$d_6$, 23 °C) spectrum of HO–PMLA$^{Be}{}_{2200}$-*b*-PHB$_{4900}$-*b*-PMLA$^{Be}{}_{2200}$–OH synthesized by ROP of MLA$^{Be}$ from Nd(OTf)$_3$/HO–PHB$_{4900}$–OH (Table 1, entry 5).

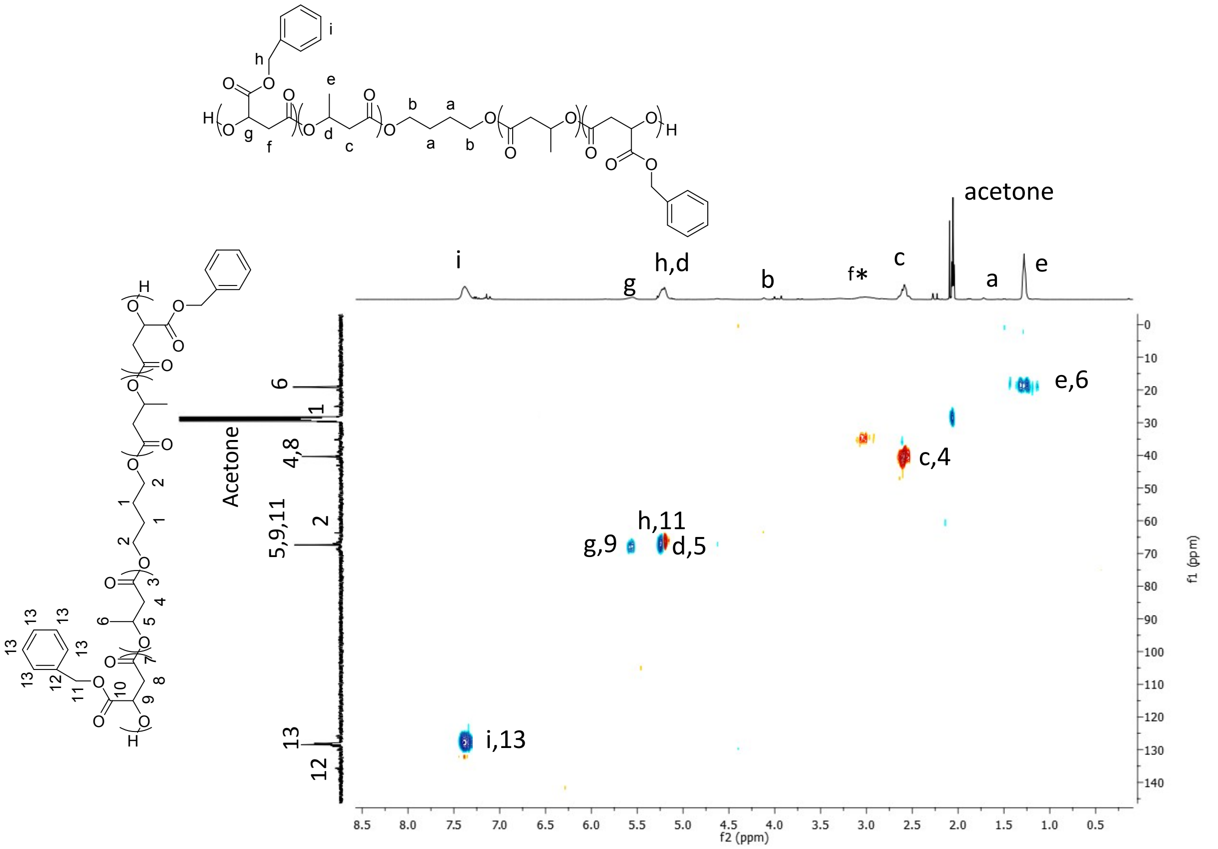

**Figure S8.** $^1$H-$^{13}$C HSQC NMR (400 MHz, acetone-$d_6$, 23 °C) spectrum of a HO–PMLA$^{Be}{}_{2200}$-*b*-PHB$_{4900}$-*b*-PMLA$^{Be}{}_{2200}$–OH sample synthesized by ROP of MLA$^{Be}$ from Nd(OTf)$_3$/HO–PHB$_{4900}$–OH (Table 1, entry 5).

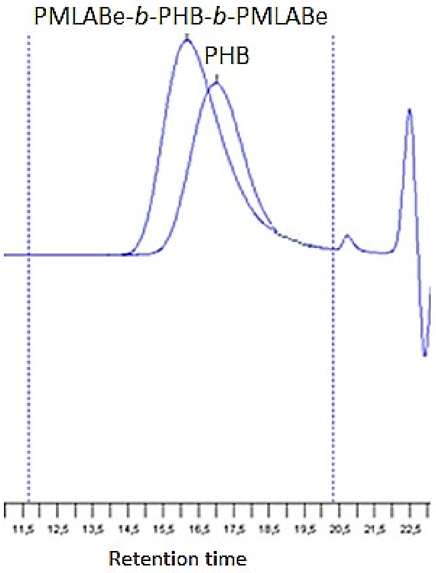

**Figure S9.** SEC chromatograms of a HO–PHB$_{4900}$–OH macroinitiator ($M_{n,SEC}$ = 5100 g.mol$^{-1}$, $Đ_M$ = 1.21; Table S1, entry 5), and of the corresponding HO–PMLA$^{Be}{}_{2200}$-*b*-PHB$_{4900}$-*b*-PMLA$^{Be}{}_{2200}$–OH triblock copolymer ($M_{n,SEC}$ = 5600 g.mol$^{-1}$, $Đ_M$ = 1.23) synthesized by the ROP of MLA$^{Be}$ promoted by the Nd(OTf)$_3$/HO–PHB$_{4900}$–OH catalytic system (Table 1, entry 5). Note that the slight tailing of the traces in the low molar mass (high retention time) region is systematically observed in the chromatograms of PHA-based homopolymers and copolymers and is inherent to the SEC apparatus; refer to C. G. Jaffredo, J.-F. Carpentier, S. M. Guillaume, *Macromol. Rapid Commun.* **2012**, *33*, 1938−1944 and [7,12c,d]

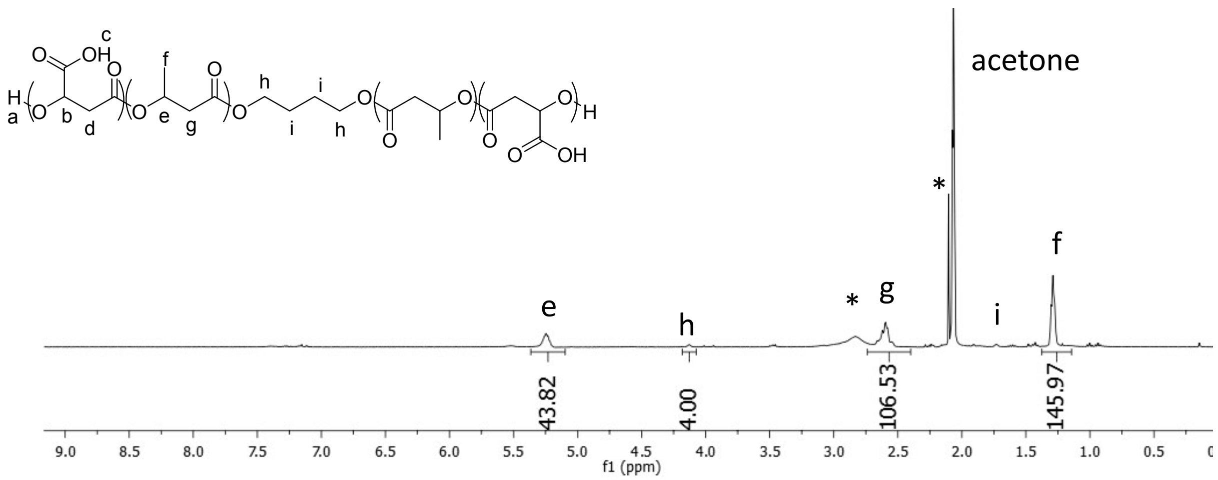

**Figure S10.** $^1$H NMR (400 MHz, acetone-$d_6$, 23 °C) spectrum of HO–PMLA$_{1100}$-*b*-PHB$_{4600}$-*b*-PMLA$_{1100}$–OH obtained upon hydrogenolysis of HO–PMLA$^{Be}{}_{2200}$-*b*-PHB$_{4900}$-*b*-PMLA$^{Be}{}_{2200}$–OH (Table 1, entry 5) (* marker stands for residual water and acetone). The signals of the PMLA block do not suitably integrate as the result of the partial solubility of this block in acetone.

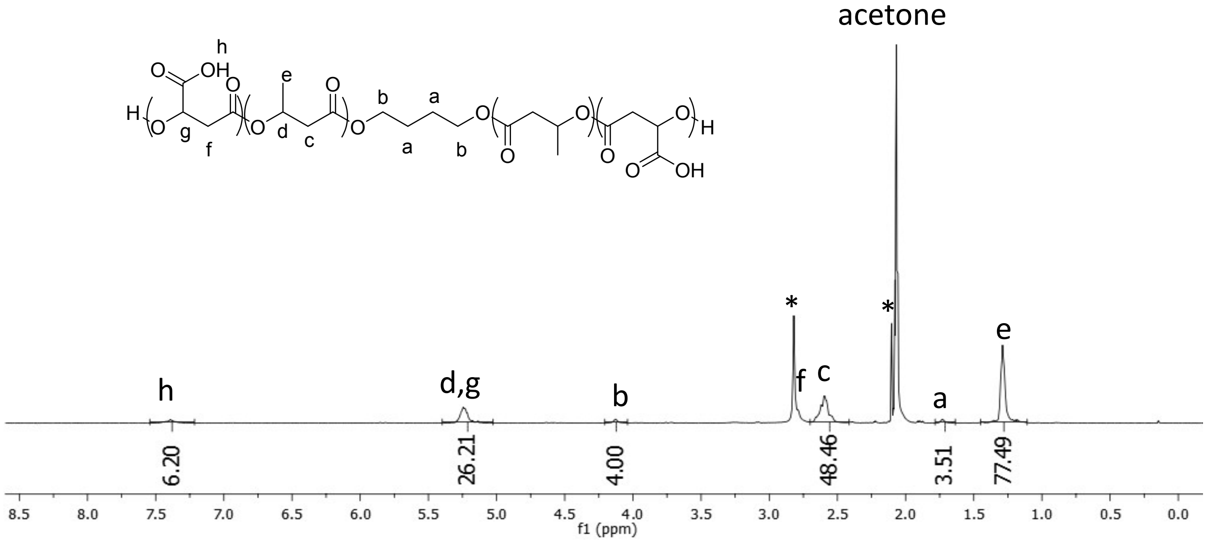

**Figure S11.** $^1$H NMR (400 MHz, acetone-$d_6$/TFA (98:02, *v*/*v*), 23 °C) spectrum of HO–PMLA-*b*-PHB-*b*-PMLA–OH obtained upon hydrogenolysis of HO–PMLA$^{Be}{}_{400}$-*b*-

PHB$_{2500}$-*b*-PMLA$^{\mathrm{Be}}_{400}$–OH (Table 1, entry 1) (* marker stands for water and residual acetone).

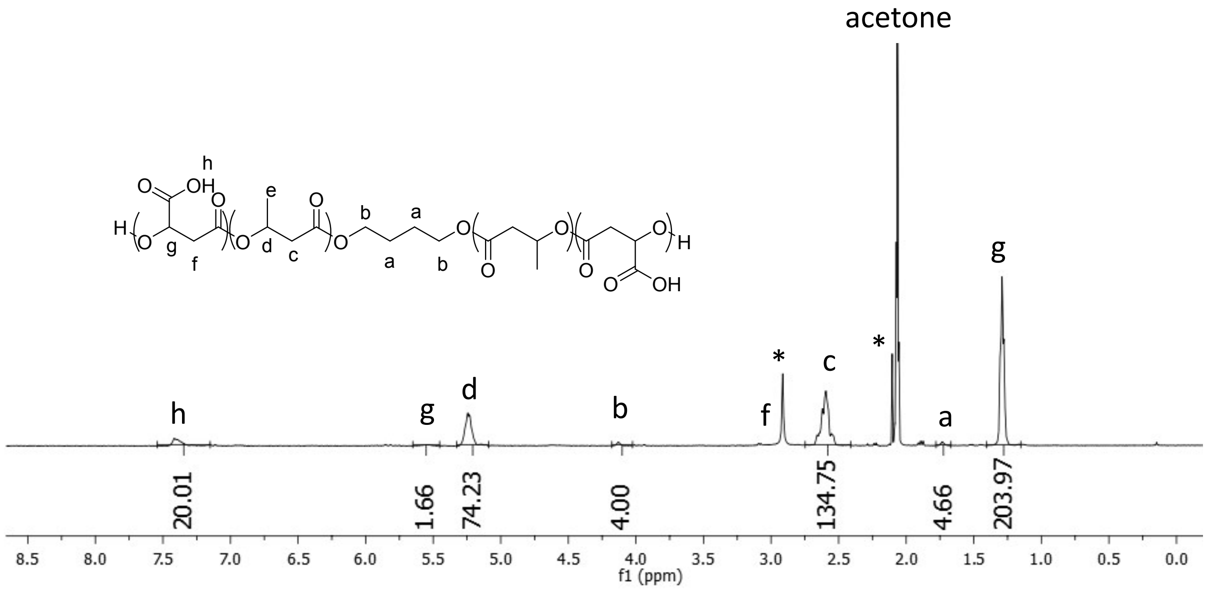

**Figure S12**. $^{1}$H NMR (400 MHz, acetone-*d$_6$*/TFA (98:02, *v*/*v*), 23 °C) spectrum of HO–PMLA-*b*-PHB-*b*-PMLA–OH obtained upon hydrogenolysis of HO–PMLA$^{\mathrm{Be}}_{500}$-*b*-PHB$_{6500}$-*b*-PMLA$^{\mathrm{Be}}_{500}$–OH (Table 1, entry 2) (* marker stands for water and residual acetone).

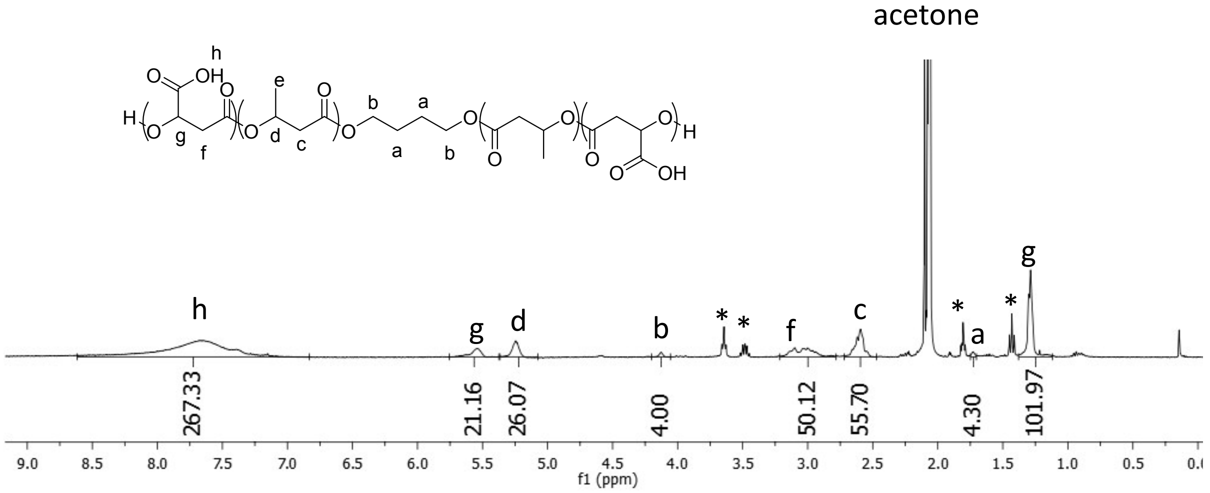

**Figure S13.** $^{1}$H NMR (400 MHz, acetone-$d_6$/TFA (98:02, *v*/*v*), 23 °C) spectrum of HO–PMLA-*b*-PHB-*b*-PMLA–OH obtained upon hydrogenolysis of HO–PMLA$^{\mathrm{Be}}{}_{4100}$-*b*-PHB$_{2500}$-*b*-PMLA$^{\mathrm{Be}}{}_{4100}$–OH (Table 1, entry 6) (* marker stands for unidentified impurities).

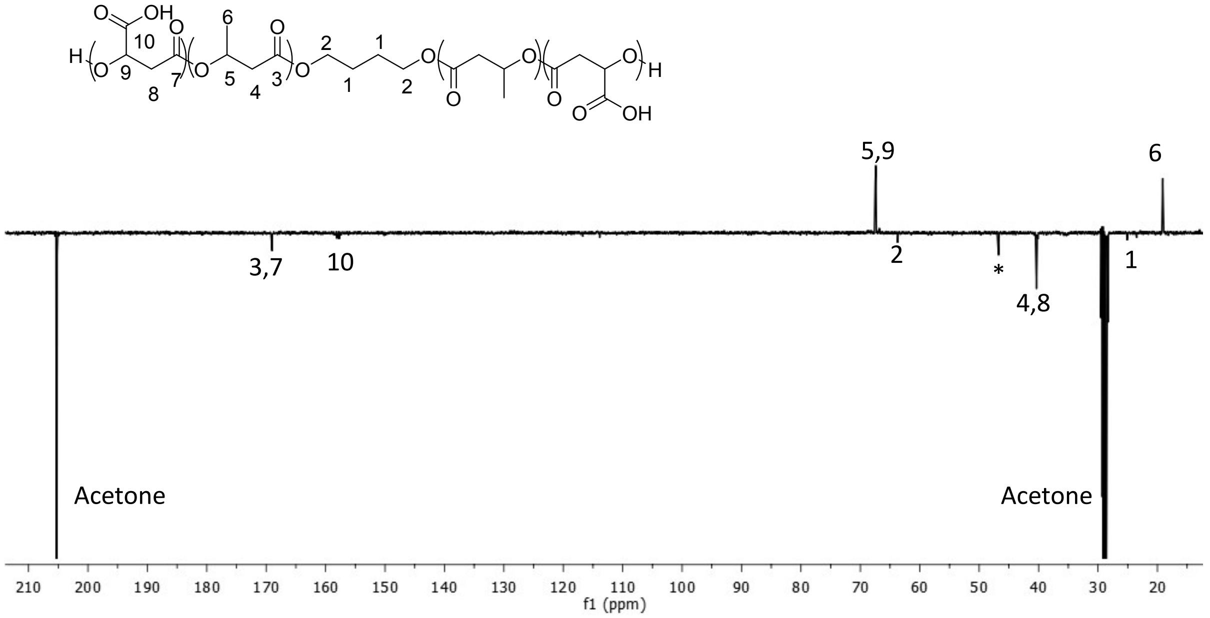

**Figure S14.** $^{13}$C{$^{1}$H} J-MOD NMR (100 MHz, acetone-$d_6$/TFA –98:02, *v*/*v*, 23 °C) spectrum of the HO–PMLA$_{1100}$-*b*-PHB$_{4600}$-*b*-PMLA$_{1100}$–OH sample obtained upon hydrogenolysis of the HO–PMLA$^{\mathrm{Be}}{}_{2200}$-*b*-PHB$_{4900}$-*b*-PMLA$^{\mathrm{Be}}{}_{2200}$–OH (Table 1, entry 5) (* marker stands for unidentified impurities).

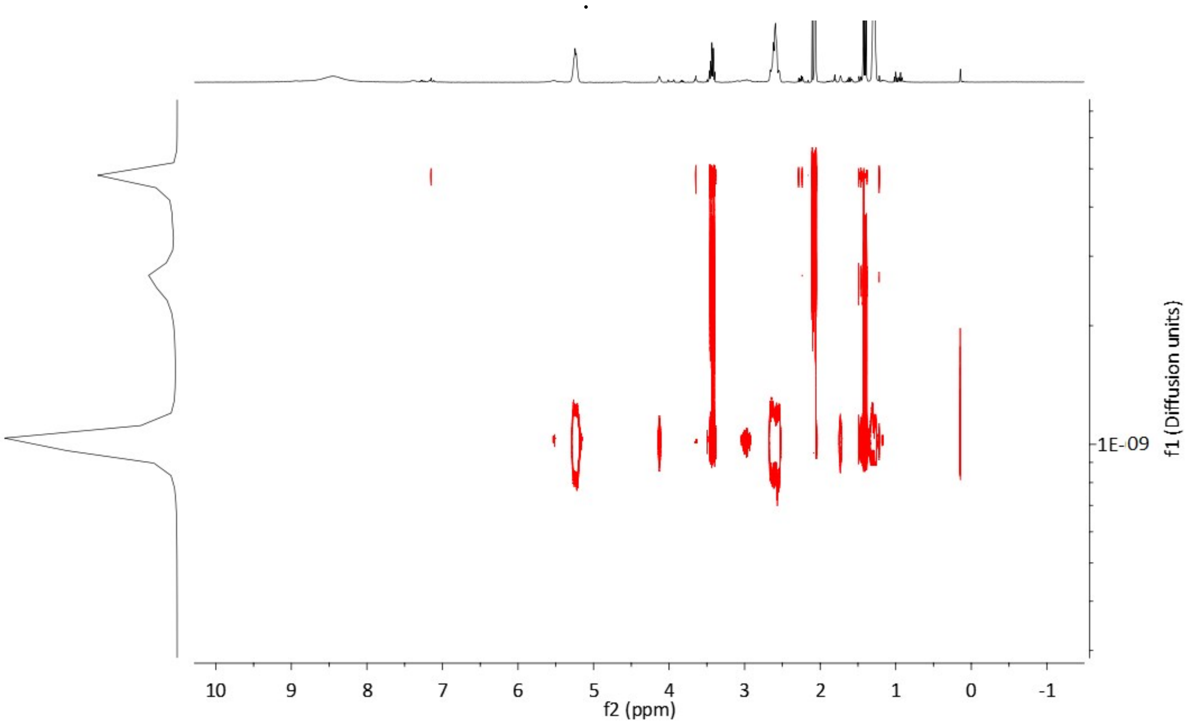

**Figure S15.** DOSY NMR (400 MHz, acetone-$d_6$, 23 °C) spectrum of HO–PMLA$_{1100}$-*b*-PHB$_{4600}$-*b*-PMLA$_{1100}$–OH obtained upon hydrogenolysis of HO–PMLA$^{Be}{}_{2200}$-*b*-PHB$_{4900}$-*b*-PMLA$^{Be}{}_{2200}$–OH (Table 1, entry 5) (D = 102.10$^{-11}$ m.s$^{-1}$).

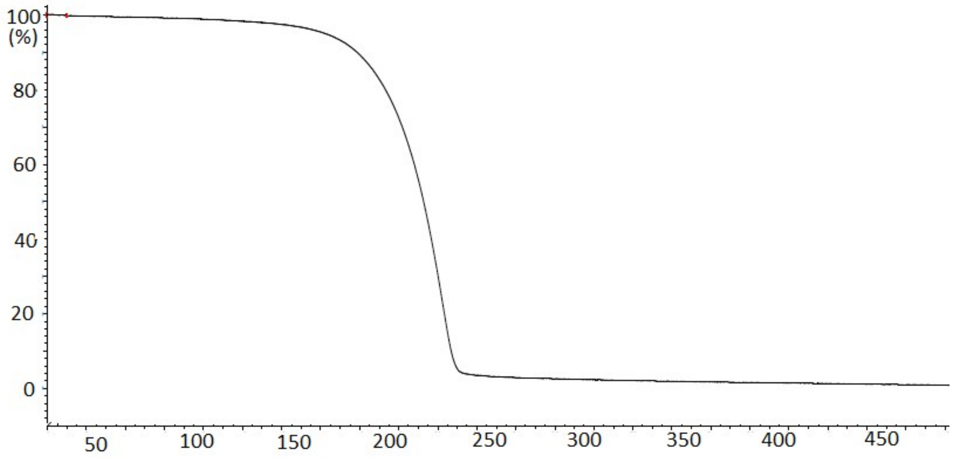

**Figure S16.** Thermal degradation profiles of PMLA$^{Be}{}_{4300}$ homolymer.

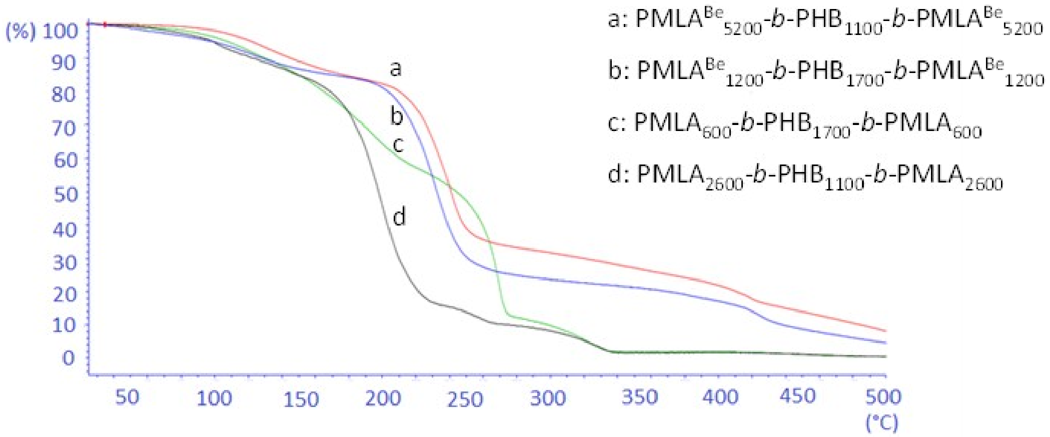

**Figure S17.** Thermal degradation profiles of PMLA-*b*-PHB-*b*-PMLA copolymers: a) PMLA$^{Be}_{5200}$-*b*-PHB$_{1100}$-*b*-PMLA$^{Be}_{5200}$, b) PMLA$^{Be}_{1200}$-*b*-PHB$_{1700}$-*b*-PMLA$^{Be}_{1200}$, c) PMLA$_{600}$-*b*-PHB$_{1700}$-*b*-PMLA$_{600}$, c) PMLA$_{2600}$-*b*-PHB$_{1100}$-*b*-PMLA$_{2600}$ (Table 1, entries 4, 7, ESI†).

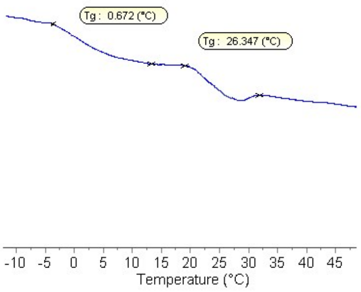

**Figure S18.** DSC trace (second heating cycle; heating rate = 10 °C.min$^{-1}$; helium flow) of PMLA$^{Be}_{5200}$-*b*-PHB$_{1100}$-*b*-PMLA$^{Be}_{5200}$ (Table 1, entry 7).

## References

---

[1] P. Guerin, J. Francillette, C. Braud, M. Vert, *Makromol. Chem., Macromol. Symp.*, 1986, **6**, 305–314.

[2] M.-A. Leboucher-Durand, V. Langlois, P. Guérin, *React. Funct. Polym.*, 1996, **31**, 57–65.

[3] A. Couffin, B. Martín-Vaca, D. Bourissou, C. Navarro, *Polym. Chem.*, 2014, **5**, 161–168.

[4] C. G. Jaffredo, J.-F. Carpentier, S. M. Guillaume, *Macromolecules,* 2013, **46**, 6765–6776.

[5] G. Barouti, C. G. Jaffredo, S. M. Guillaume, *Polym. Chem.*, 2015, **6**, 5851–5859.

[6] G. Barouti, A. Khalil, C. Orione, K. Jarnouen, S. Cammas-Marion, P. Loyer, S. M. Guillaume, *Chem. Eur. J- A European J.* 2016, **22**, 2819 –2830.

[7] G. Barouti, K. Jarnouen, S. Cammas-Marion, P. Loyer, S. M. Guillaume, *Polym. Chem.* 2015, **6***,* 5414–5429.

[8] M. Helou, G. Moriceau, Z. W. Huang, S. Cammas-Marion, S. M. Guillaume, *Polym. Chem.*, 2011, **2**, 840–850.